UCRL- 95981
PREPRINT

Laser-Plasma-Interaction Experiments Using Multikilojoule Lasers

R. P. Drake
Lawrence Livermore National Laboratory
University of California
Livermore, CA 94550

This paper was prepared for submittal to
Laser and Particle Beams
Proceedings of the 18th European Conference
on Laser Interaction with Matter
Prague, Czechoslovakia
May 4-8, 1987

July, 1987

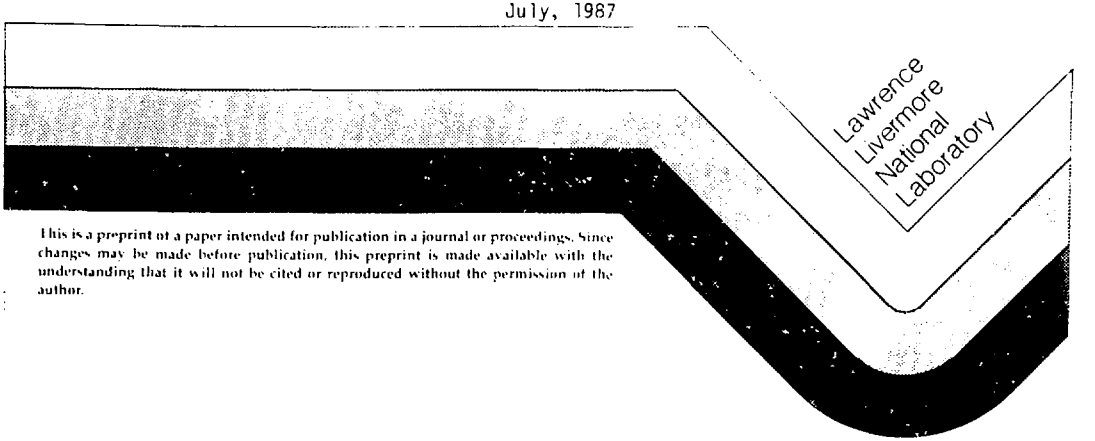

Laser-Plasma-Interaction Experiments Using Multikilojoule Lasers*

R. Paul Drake

Lawrence Livermore National Laboratory
University of California
Livermore, CA USA 94550

UCRL--95981

DE87 013483

Abstract

This paper summarizes the results of several laser-plasma-interaction experiments using multikilojoule lasers, and considers their implications for laser fusion. The experiments used 1.06, 0.53, 0.35, and 0.26 μm light to produce relatively large, warm, planar plasmas and to study the effect of laser wavelength and density-gradient scale length on the Stimulated Raman Scattering and on the scattering of light at frequencies near the incident laser frequency by Stimulated Brillouin Scattering or other processes. The results of these experiments suggest that some laser wavelength between 0.2 and 0.6 μm will be required for high-gain laser fusion.

Introduction

For laser fusion to succeed, the interaction processes in the laser-produced plasma must absorb the laser light efficiently and produce few suprathermal electrons. As the energy and duration of the laser irradiations increase, the plasmas they produce develop longer scale lengths and become more planar. During the 1980's, multikilojoule lasers have allowed the study of laser-plasma-interaction processes in plasmas that could not have been produced with smaller lasers. This paper summarizes some laser-plasma-interaction experiments performed at the Lawrence Livermore National Laboratory in recent years, with emphasis on results that directly affect the prospects for laser fusion.

To motivate this discussion, consider what conditions can be produced by a high-power laser that is able to irradiate a target with more than 1 kJ of energy. The irradiation can satisfy three conditions that cannot be simultaneously met using smaller lasers. First, the intensity (I_L) can exceed 10^{15} W/cm^2. This is near the upper limit envisioned for laser fusion. Second, the pulse duration (τ) can equal or exceed 1 ns. This is long enough to allow a large corona to develop in front of a target although it does not equal the 5 to 10 ns pulse durations that will be needed for high-gain laser fusion. Third, the spot diameter can exceed 300 μm, with effects described shortly. Given these irradiation conditions, the plasma produced will have these properties: First, it will have an electron temperature greater than 1 keV. Such temperatures are comparable to those anticipated in high gain targets. Second, it will remain relatively planar throughout a 1 ns

laser pulse because the spot size is larger than $c_s\tau$, where c_s is the ion sound speed in the plasma. High gain targets are expected to produce relatively planar plasmas. Third, it will reach density gradient scale lengths (L) of several hundred laser wavelengths (λ) or more, where $L \equiv [(1/n)\ dn/dx]^{-1}$. These scale lengths are smaller than those expected in high-gain targets, where L/λ will reach several thousand. However, they can be used for significant experiments, as is shown next.

By producing the conditions just discussed, multikilojoule lasers can perform two useful types of experiment. First, they can identify mechanisms of laser-plasma interaction that appear in planar plasmas at intensities and temperatures of interest to laser fusion. The most obvious example of this is sidescatter processes, which are not strongly favored in the spherical plasmas produced at relevant intensities by smaller lasers. Second, they can study the dependence of any interaction mechanism on the scale length, L. Such experiments hope to learn enough to extrapolate with confidence to the scale lengths anticipated in high-gain targets. We note that one must reach values of L/λ that significantly exceed 100 to exceed the thresholds or achieve significant gain for several interaction mechanisms of interest. [Max et al. 1984] In addition, by performing such experiments using several laser wavelengths, one can study the wavelength scaling of the important mechanisms.

In this work, we discuss measurements of the light scattered out of the target plasma in two ranges of frequency. After the description of the experiments themselves, which is next, we discuss measurements of light scattered with frequencies near the fundamental frequency of the

laser light (ω_0). Such light may be reflected from critical density (n_c) or may be scattered directly by Stimulated Brillouin Scattering, [Tang 1966, Liu et al. 1974, Thomson and Kruer 1978], in which the incident light wave decays into a scattered light wave and an ion-acoustic wave. It may be indirectly produced as a result of resonance absorption, [Freidberg et al. 1972, Speziale and Catto 1977], in which resonantly-driven plasma waves near the critical density absorb (and may re-remit) light, or by parametric decay, [Perkins and Flick 1971], in which the incident light wave decays into an ion-acoustic wave and an electron-plasma wave. We follow the discussion of scattering at frequencies near ω_0 with a discussion of scattering at frequencies below ω_0 but above $\omega_0/2$. Light is scattered into these frequencies by Stimulated Raman Scattering [Liu et al. 1974] in which the incident light wave decays into a scattered light wave and an electron-plasma wave. We ignore the light scattered at $\omega_0/2$, by two-plasmon decay [Jackson 1967, Langdon et al. 1979] or by Raman scattering at 0.25 n_c, because the evidence indicates that, in large plasmas, the scattering by SRS at densities below 0.25 n_c overwhelms this scattering, both as a source of hot electrons and of scattered light, and because there is no reason to expect this trend to change in the larger plasmas of high-gain targets. Finally, in the conclusion, we summarize the results and consider their implications for laser fuison.

The Experiments

Several laser facilities were used for the experiments discussed here. These are summarized in Table 1. Argus [Rosen et al. 1979] and Shiva [Phillion et al. 1982a, Phillion et al. 1982b] produced results using 1.06 μm laser light. The Novette facility irradiated targets with 0.53 μm light [Drake et al. 1984, Drake et al. 1986] and 0.26 μm light [Turner et al. 1985]. The Nova facility produced the results discussed here for 0.35 μm light. As the table shows, the energy on target was typically 2 kJ but varied from less than 1 kJ to about 4 kJ. When possible, the experiments used only one laser beam so that the results could be interpreted most clearly. However, experiments using Shiva required 10 beams.

All these lasers used Nd-doped glass to amplify a low-energy pulse of light, and they all operated with narrow bandwidth. The wavelengths shorter than 1 μm were produced by harmonic conversion of the 1 μm light. In every case, the intensity at the target plane was strongly modulated, with peak-to-valley fluctuations of order 5 to 1.

The laser pulses were usually Gaussian in shape, and varied from 700 ps to 2 ns in FWHM. The Nova pulses for the results discussed here were square, 1 ns pulses. A few experiments have found no strong dependence on pulse shape or duration over this range, so we ignore differences in pulse shape during the discussion that follows.

The data that follows were obtained by irradiating two types of targets. Some targets were thick enough that they did not burn through during the laser pulse. We refer to these as "disk" targets. Most of the disk targets were gold, although some low-Z disk targets have been

used. The experiments using disk targets produced local gradient scale lengths, L, of several hundred laser wavelengths. We refer to the other type of target as a "foil" target. These targets are thin enough to burn through during the laser pulse. The expanding plasma that results has a density maximum and may have a significant volume over which L exceeds 1,000 laser wavelengths. We have extensive data from CH foils, and some data from Au foils.

In the following, results from foil and/or disk targets irradiated with about 2 kJ of energy are compared to results from disk targets irradiated with about 100 J, in order to identify the effects of scale length and planarity on the laser-plasma interactions.

The results discussed in this work were obtained with laser intensities of order 2×10^{15} W/cm^2. We have performed some experiments to study the scaling of the laser-plasma-interaction processes with laser intensity. Although we will mention some of the results in the following, they are in general beyond the scope of this paper. Many diagnostics were used to measure the scattered light emitted by these plasmas, and to measure the hard x rays produced by the suprathermal electrons. These diagnostics are described in detail in the reports of the individual experiments cited above. In general, they included absolutely-calibrated photodiodes to measure the fluence and angular distribution of the scattered light, spectrometers coupled to streak cameras to measure the time-resolved spectra of the scattered light, and absolutely calibrated x-ray spectrometers to measure the hard x rays. Other diagnostics contributed to various individual experiments.

Scattering Near ω_0

We now present and discuss measurements of the scattered light with frequencies near the frequency of the light incident on target, ω_0. The results of long-scale-length and wavelength-scaling experiments might have been either favorable or unfavorable for laser fusion. On the one hand, longer scale-length plasmas will absorb a larger fraction of the laser light before it reaches the critical surface. This will reduce the reflection of laser light from the critical surface and the hot electron production by resonance absorption. In addition, other interaction processes may be collisionally damped (or just overwhelmed by inverse-bremsstrahlung absorption) at shorter laser wavelengths.

On the other hand, long scale length, planar plasmas should have significant gain for Stimulated Brillouin Scattering (SBS) backscatter and sidescatter, so that the absorption of laser light could become much less efficient. Of particular concern is any convective process that scales as exp (β), where $\beta \propto I_L L$. Any such process that is detectable in multikilojoule experiments has the potential to be devastating at the multimegajoule level.

Long-scale-length, planar plasmas have produced SBS sidescatter. Figure 1 provides one example. It shows the fluence of the scattered light, in J/Sr, as a function of azimuthal angle about the axis of propagation of the laser beam. Data is shown for polar angles of 120° and 135° with respect to the direction of propagation. The experiment that produced this data used 2 kJ of 0.53 μm light to irradiate a 660 μm spot on a gold disk for 1 ns, producing an average intensity of

6×10^{14} W/cm^2. The laser beam was incident along the target normal. The figure shows that the scattering perpendicular to the electric-field vector of the incident light (out-of-plane) is many times stronger than the in-plane scattering. This dependence is expected for SBS sidescatter and is not expected for any other mechanism at these frequencies.

We have now observed SBS sidescatter from plasmas produced with 1, 0.53, and 0.35 μm light (and did not attempt to observe it with 0.26 μm light). Experiments at similar laser intensities and pulse lengths, but using smaller spots, have not seen this process. Thus, it is a scattering mechanism that appears in relatively long-scale-length, planar plasmas. The magnitude of the SBS sidescatter, integrated over polar angle from 90° to 150°, has been as large as 10% of the laser energy. Thus, this can be a significant energy loss mechanism and its scaling to high-gain conditions is of concern to laser fusion. Fortunately, the SBS sidescatter has been observed to saturate quite strongly as a function of laser intensity. As a result, the best projection is that it will not substantially exceed 10% of the laser energy even under high-gain conditions.

The backscattered light with frequencies near ω_0 may result from SBS backscatter, reflection from critical, or other more complex processes. We have not carried out sufficiently detailed spectroscopic studies to determine which mechanisms dominate under what conditions. We have measured the total fraction of the incident laser energy that is backscattered, and it is smaller from 2 kJ experiments than it is from 100 J experiments.

The net effect of smaller backscatter and the advent of sidescatter is that the total amount of scattering at frequencies near ω_0 has changed little as scale-length has increased. This is illustrated in Table 2. (The "100 J Laser" results in Table 2 were obtained using Argus [Campbell, 1981].) At the two wavelengths for which there is data, the difference between the experiments with different scale lengths is less then the relevant uncertainties. We view this scaling of the total scattered light as scale length increases with cautious optimism. It leads us to hope that the total scattering will not increase significantly in high-gain targets with larger plasmas.

The scaling of the scattered light with laser wavelength is much more favorable. The total scattered light decreases as wavelength decreases, as Table 2 also shows. In addition, both the backscattered energy and the SBS sidescatter are observed to decrease. Inverse bremsstrahlung absorption definitely is larger in the denser, cooler plasmas produced by the shorter-wavelength lasers, and more absorption takes place at lower densities. Furthermore, any light that is scattered is more strongly absorbed as it leaves the plasma. Moreover, other collisional affects might also act to decrease the scattering. Thus, these wavelength-scaling data are both sensible and encouraging. If the mechanisms were more clearly understood, we would expect to conclude that scattered light at frequencies near ω_0 would not prevent high-gain laser fusion, particularly for laser wavelengths of 0.53 μm or less.

Data from the foil targets were excluded from Table 2 for two reasons. First, the foil targets produce long density-gradient scale lengths but relatively short velocity-gradient scale lengths. As SBS

requires long scale lengths of both density and velocity gradients, such targets should produce little SBS. Second, and as one thus expects, we observe very little scattering at frequencies near ω_0 after such targets have burned through. The velocity-gradient scale lengths of such targets at very low densities ($n \leq 0.05\ n_c$) are quite large after burnthrough, however. Thus, this result shows that the dominant region of SBS from such plasmas is at densities above $0.05\ n_c$, which is also encouraging.

Stimulated Raman Scattering

The possibilities for Stimulated Raman Scattering (SRS) are similar to those for SBS. First, increasingly planar, long-scale-length plasmas may allow more growth of SRS backscatter and sidescatter. Second, collisional damping may quench SRS. Finally, it is important to examine the saturation behavior of SRS.

We have observed SRS sidescatter from targets irradiated at all the laser wavelengths included in Table 1. High-Z and low-Z disk and high-Z and low-Z foil targets have all produced such scattering. The expected strong difference between out-of-plane scattering and in-plane scattering has been observed for 0.53 and 0.35 μm irradiations. (Sufficiently detailed measurements were not carried out for 1.06 and 0.26 μm). Figure 2 shows some data from the irradiation of a gold disk target with 0.53 μm light. The experimental geometry is the same as that described for Fig. 1. The figure shows the strongly out-of-plane scattering observed at 120° and 135° from the direction of propagation of the laser

beam. Based on the measured spectrum, this light was probably scattered at angles near 90° within the plasma, after which refraction steered it to the observed angle.

We also have observed increasing SRS backscatter from longer-scale-length plasmas. Figure 3 illustrates the increase of the total amount of SRS for gold targets irradiated with 0.53 μm light at an intensity of about 2×10^{15} W/cm^2. This figure shows the fraction of the laser energy scattered as SRS light as a function of normalized gradient scale-length, L/λ. Experiments on Argus, with small scale lengths and relatively spherical plasmas, produced SRS fractions of about 10^{-4}. The relatively planar and larger-scale-length plasmas of the Novette experiments produced SRS fractions of order 10^{-2} for disk targets and 10^{-1} for foil targets. It is unclear from the existing data at what level the SRS will saturate as scale length increases. Given that high-gain targets will produce plasmas with scale lengths significantly larger than those shown in the figure, this question is of some concern for laser fusion.

Fortunately, it is possible to control SRS by means of collisional damping. Figure 4 shows the SRS fraction as a function of the collisional-damping parameter, ν_{ei}/γ_o where ν_{ei} is the electron-ion collision frequency and γ_o is the homogeneous growth rate for SRS. The data is from foil targets irradiated at an intensity of about 10^{15} W/cm^2. This figure includes data from CH and Au foils irradiated at various wavelengths. Experiments near or below the collisional damping threshold, [Estabrook and Kruer 1984], $\nu_{ei}/\gamma_o \sim 1$, produced negligible amounts of SRS. We have also observed a very strong

dependence of the SRS fraction on intensity in experiments near the collisional-damping threshold.

The wavelength and scale-length dependence of SRS is illustrated in Table 3. (The "100 J Laser" results in Table 3 are from high-Z targets irradiated with 1.06 μm light [Phillion it al. 1982], or 0.53 μm light [Turner et al. 1983] using Argus, and from low-Z targets irradiated with 0.35 μm light using GDL [Tanaka et al. 1982].) The SRS fraction depends quite dramatically on scale-length, as was discussed earlier. However, at all wavelengths longer than 0.26 μm, the SRS fraction is independent of wavelength within the experimental uncertainties. Three observations are relevant here. First, the effects of the decrease in $I_L \lambda^2$ from 1.06 to 0.35 μm is apparently offset by the effects of the increase in L/λ. As a result, there is no substantial change in the SRS fraction. Second, the SRS responds much less to changes in wavelength (and consequent increases in inverse bremsstrahlung absorption) than SBS does. This suggests that SBS occurs at higher densities than SRS. Third, the decrease in the amount of SRS from the CH foil at 0.26 μm might be an effect of inverse bremsstrahlung absorption.

We have also observed the hard x rays produced as a result of SRS. This observation was by means of the bremsstrahlung x rays emitted by such electrons when they slow down in a target. The amount, temperature, and timing of these hot electrons was in quantitative agreement with the expected production of hot electrons by the plasma waves that grow during SRS [Drake et al. 1984, Drake et al. 1986].

In summary of the SRS data, we have observed these trends: SRS sidescatter develops in large plasmas; the total amount of SRS increases as the gradient scale-length, L, increases; the amount of SRS is not a strong function of the irradiating wavelength; SRS can be quenched by collisional damping; and the saturation level of SRS in the absence of collisional damping is not known.

Conclusion

During the 1980's, we have produced relatively large, warm, planar plasmas using multikilojoule lasers operating at four different wavelengths. Although the pulse lengths and scale lengths are not as large as those that will exist in a high-gain, laser-fusion target, they are large enough to exceed thresholds or provide substantial gain for several interaction processes that are sensitive to gradients in the plasma. One hopes that experiments using such plasmas will allow one to extrapolate with confidence to high-gain conditions.

The experiments have indeed produced new effects and some clear trends. Backscatter and sidescatter at frequencies near ω_0 are present, but their strong saturation with laser intensity and their significant reduction as laser wavelength decreases lead one to believe that, at some laser wavelength from 0.26 to 0.53 μm, SBS will not prevent laser fusion from working. One minor mystery that does remain is that it appears that SBS does not take place at densities well below 0.25 n_c.

It is now clear that SRS and the consequent hot-electron production can be controlled by collisional damping, although this may necessitate some undesireable design tradeoffs in some types of laser-fusion

targets. It is not yet clear at what level the SRS will saturate, in the absence of collisional damping. This last issue remains a fruitful topic for further experimentation.

With regard to the effect of interaction mechanisms in the underdense plasma on the prospects for laser fusion, one can say several things. First, the plasmas produced and studied using multikilijoule lasers are large enough and planar enough that we have found evidence of every process that is expected, from theoretical considerations, to be present in a high-gain target (except for filamentation which is probably present and undetected).

Second, and based on the available data, no known process (including two plasmon decay, forward Raman and resonance absorption, which were not discussed here) scales in such a way that it definitely prevents laser fusion from working for laser wavelengths well below 1 μm.

Third, and based on present knowledge, the effects of interaction mechanisms in the underdense plasma are not negligible. They appear likely to affect the choice of driver wavelength, laser intensity, and laser-beam smoothness or bandwidth, as well as the details of target design.

In conclusion, the case for the viability of laser fusion is much more complete than it was in 1980. However, the case for any specific driver and target design is not yet complete. To have maximum impact on ICF, future research should focus on the issues now remaining to place more definite constraints on the properties of the driver and target.

Acknowledgements

The author is indebted to the many individuals who carried out the experiments and analysis summarized here, and who appear as authors in the papers listed below under Rosen, Phillion, Drake, and Turner, and in addition to the larger number of individuals in laser operations, target fabrication, target diagnostics, and plasma theory who worked to support these experiments during the past decade. Additional contributors to the experiments on Nova that have not yet appeared in print include P.E. Young, C.B. Darrow, and D.L. Montgomery of LLNL and H.A. Baldis of NRC Canada. Of particular value to the author's understanding were discussions with Drs. E.A. Williams, R.E. Turner, W.L. Kruer, D.W. Phillion, E.M. Campbell, Kent Estabrook, and B.F. Lasinski of LLNL and T.W. Johnston of INRS-Energie. Of course, any errors in the manuscript are the sole responsibility of the author.

---

*Work performed under the auspices of the U.S. Department of Energy by the Lawrence Livermore National Laboratory under contract number W-7405-ENG-48.

References:

CAMPBELL, E.M. 1981, private communication.

DRAKE, R.P., TURNER R.E., LASKINSKI, B.F., et al. 1984 Phys. Rev Lett. 53, 1739.

DRAKE, R.P., TURNER, R.E. LASINSKI, B.F., WILLIAMS, E.A., PHILLION, D.W., ESTABROOK, K.G., CAMPBELL, E.M., JOHNSTON, T.W., MANES, K.R., HILDUM, J.S. 1986 submitted to Phys. Fluids.

ESTABROOK, KENT and KRUER, W.L. 1984 Phys. Rev. Lett. 53, 465.

FREIDBERG, J.P., MITCHELL, R.W., MORSE, R.L., et al. 1972 Phys. Rev. Lett. 28, 795.

JACKSON, E.A. 1967 Phys. Rev. 153, 235.

LANGDON, A.B. LASINSKI, B.F. KRUER, W.L. 1979 Phys. Rev. Lett. 43, 133.

LIU, C.S., ROSENBLUTH, R.B., WHITE, R.B. 1974 Phys. Fluids 17, 1211.

MAX, C.E., CAMPBELL, E.M., MEAD, W.C., KRUER, W.L., PHILLION D.W., TURNER, R.E., LASINSKI, B.F. and ESTABROOK, K.G. 1984 p. 507 in "Laser Interaction and Related Plasma Phenomena", Vol. 6, Ed. by Heinrich Hora and George H. Miley, Plenum.

PERKINS, F.W. and FLICK, J. 1971 Phys. Fluids 14, 2012.

PHILLION, D.W., BANNER, D.L., CAMPBELL, E.M., TURNER, R.E., ESTABROOK, K.G. 1982a Phys. Fluids 25, 1434.

PHILLION, D.W., CAMPBELL, E.M., EXTABROOK, K.G., PHILLION, G.E., ZE, F. 1982b Phys. Rev. Lett. 49, 1405.

ROSEN, M.D., PHILLION, D.W., RUPERT, V.C., MEAD, W.C., KRUER, W.L., THOMPSON, J.J., KORNBLUM, H.N., SLIVINSKY, V.W., CAPORASO, G.J., BOYLE, M.J., and TIRSELL, K.G. 1979 Phys. Fluids 22, 2020.

SPEZIALE, THOMAS, and CATTO, P.J., 1977 Phys. Fluids 20, 990.

TANAKA, K., BOLDMAN, L.M., SEKA, W., RICHARDSON, M.C., SOURES, J.M., WILLIAMS, E.A. 1982 Phys. Rev. Lett. 48, 1179.

TANG, C.L. 1966 J. Appl. Phys. 37, 2945.

THOMSON, J.J., and KRUER, W.L. 1978 Comm. Plasma Phys. Cont. Fusion 4, 13.

TURNER, R.E., PHILLION, D.W., CAMPBELL, E.M., ESTABROOK, K.G. 1983 Phys. Fluids 26, 579.

TURNER, R.E., ESTABROOK, K.G., KAUFFMAN, R.L., BACH D.R., DRAKE, R.P., PHILLION, D.W., LASINSKI, B.F., CAMPBELL, E.M., KRUER, W.L., WILLIAMS, E.A. 1985 Phys. Rev. Lett. 54, 189.

Figure Captions

1. The fluence (J/Sr) of the scattered ω_o light is shown as a function of azimuthal angle with respect to the direction of propagation of the laser beam, for two polar angles. The observed scattering is much stronger in the out-of-plane direction.

2. The fluence (J/Sr) of the SRS light is shown as a function of azimuthal angle with respect to the direction of propagation of the laser beam, for two polar angles. The obseved scattering is much stronger in the out-of-plane direction.

3. The fraction of the laser energy scattered as SRS light is shown as a function of the scale length of the electron-density gradient. The amount of SRS increases strongly with scale length.

4. The fraction of the laser energy scattered as SRS light is shown as a function of the collisional-damping parameter, which is the ratio of the electron-ion collision frequency to the homogeneous SRS growth rate. These data were obtained using four different laser wavelengths to produce long-scalelength plasmas from CH or Au exploding-foil targets. SRS is quenched as the damping parameter approaches 1.

THE HARDWARE

LASER	NO. OF BEAMS USED	ENERGY (kJ)	WAVELENGTH (μm)
Argus	1	0.5 - 1	1.06
Shiva	10	3 - 4	1.06
Novette	1	3 - 4	0.53
Nova	1	1.5 - 2	0.35
Novette	1	1 - 1.5	0.26

TABLE 1

Scattered Light Near the Fundamental Frequency of the Incident Laser Light

Incident Wavelength (μm)	"100 J" Lasers Gold Disks	"2 kJ" Lasers Gold Disks
1.06	60%	60%
0.53	30%	25%
0.35	Not Measured	15%

TABLE 2

The Amount of Raman-Scattered Light

Incident Wavelength (μm)	"100 J" Lasers Gold Disks	"2 kJ" Lasers Gold Disks	"2 kJ" Lasers CH Foils
1.06	0.02%	1%	10%
0.53	0.01%	1%	10%
0.35	0.01%	1%	3%
0.26	Not Measured	0.07%	2%

TABLE 3

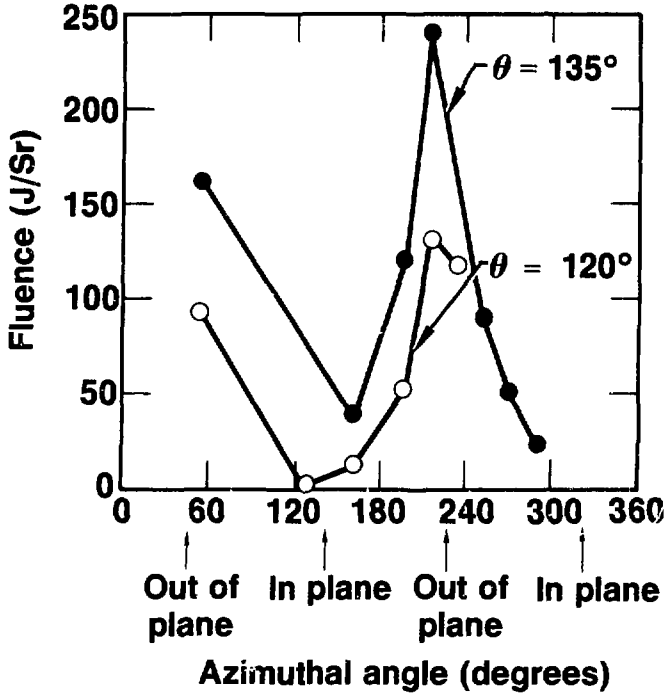
250
200
150
100
50
0
Fluence (J/Sr)
θ = 135°
θ = 120°
0
60
120
180
240
300
360
Out of plane
In plane
Out of plane
In plane
Azimuthal angle (degrees)

Figure 1

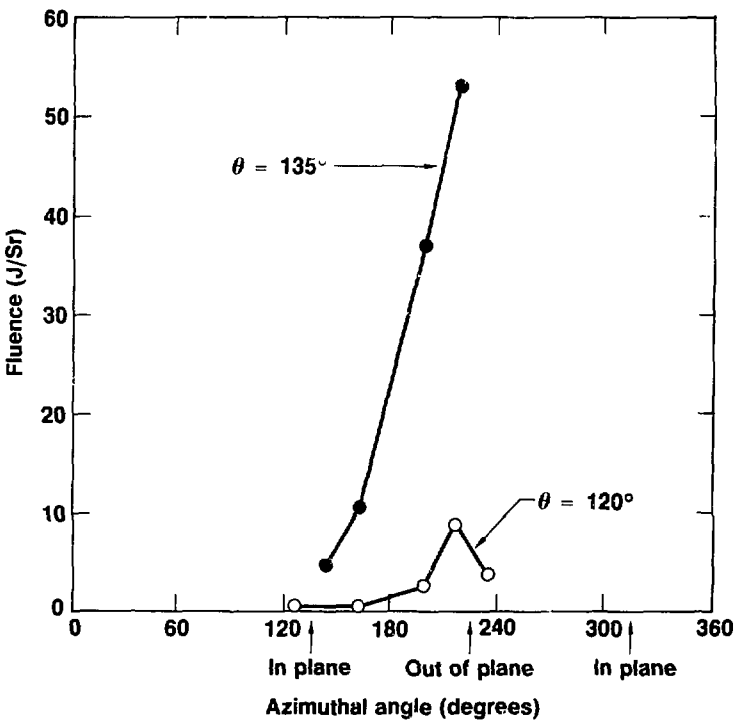
60
50
40
30
20
10
0
Fluence (J/Sr)
θ = 135°
θ = 120°
0
60
120
180
240
300
360
In plane
Out of plane
In plane
Azimuthal angle (degrees)

Figure 2

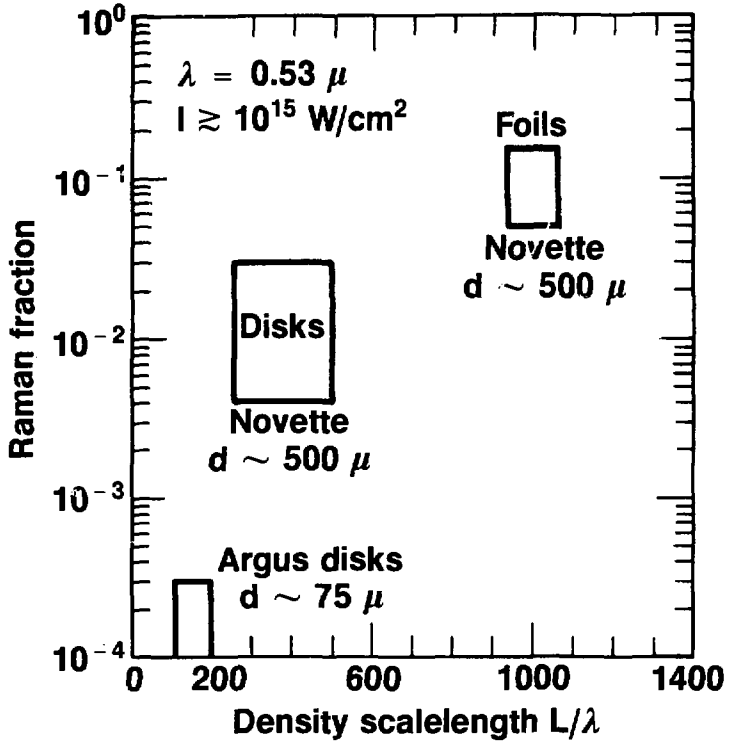
10^0
λ = 0.53 μ
I $\gtrsim 10^{15}$ W/cm^2
Foils
Novette
d ~ 500 μ
Disks
Novette
d ~ 500 μ
Argus disks
d ~ 75 μ
10^{-1}
10^{-2}
10^{-3}
10^{-4}
Raman fraction
0
200
600
1000
1400
Density scalelength L/λ

Figure 3

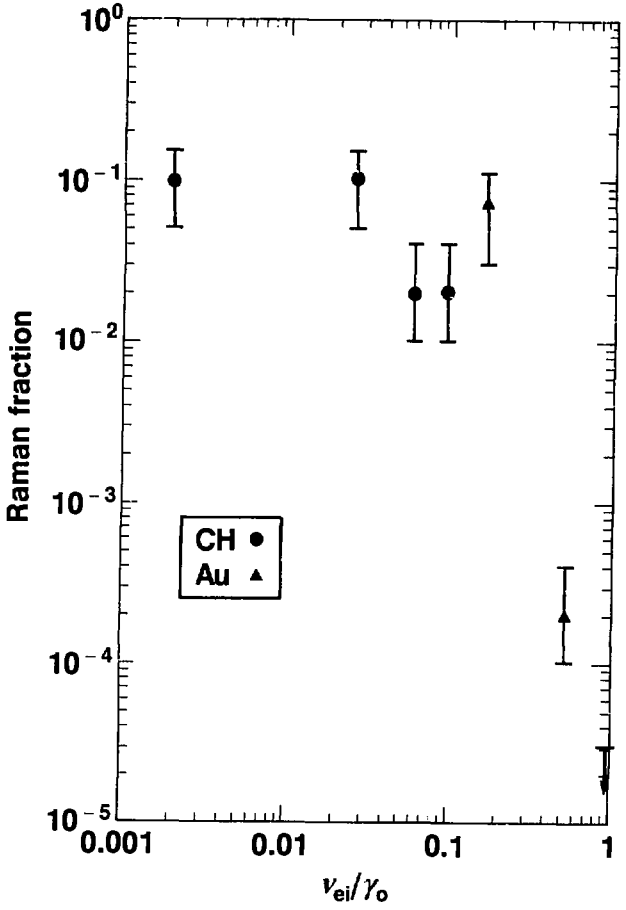
Raman fraction
10^0
10^{-1}
10^{-2}
10^{-3}
10^{-4}
10^{-5}
CH ●
Au ▲
0.001
0.01
0.1
1
ν_{ei}/γ_o

Figure 4